

B anomalies with unparticles

Jong-Phil Lee*

Sang-Huh College, Konkuk University, Seoul 05029, Korea

Abstract

We analyze the *B* anomalies associated with the $B \rightarrow D^{(*)}\tau\nu$ decays in the unparticle model. The fraction of the branching ratios $R(D^{(*)})$ and other parameters related to the polarization are fitted to the experimental data by minimizing χ^2 . The best-fit values are $R(D)_{\text{best}} = 0.371$ and $R(D^*)_{\text{best}} = 0.266$ which are still larger than the standard model predictions. We find that our results safely render the branching ratio $\text{Br}(B_c \rightarrow \tau\nu)$ below 10%.

arXiv:2012.11852v1 [hep-ph] 22 Dec 2020

* jongphil7@gmail.com

I. INTRODUCTION

Flavor physics plays an important role in particle physics to probe new physics (NP) as well as to test the standard model (SM). The SM has been very successful to describe the nature so far, and no explicit evidence for the NP has been observed yet. But the SM is incomplete in many respects and we anticipate the appearance of the NP. Recently some anomalies appear in B physics. Especially the fraction of ($\ell = e, \mu$)

$$R(D^{(*)}) \equiv \frac{\text{Br}(B \rightarrow D^{(*)}\tau\nu)}{\text{Br}(B \rightarrow D^{(*)}\ell\nu)} , \quad (1)$$

shows a tension with the SM predictions [1]

$$\begin{aligned} R(D)_{\text{SM}} &= 0.299 \pm 0.003 , \\ R(D^*)_{\text{SM}} &= 0.258 \pm 0.005 . \end{aligned} \quad (2)$$

Experimental data up to now favor larger values of the fraction [2–11]. The world averages by the Heavy Flavor Averaging Group(HFLAV) Collaboration are [12]

$$\begin{aligned} R(D)_{\text{HFLAV}} &= 0.340 \pm 0.027 \pm 0.013 , \\ R(D^*)_{\text{HFLAV}} &= 0.295 \pm 0.011 \pm 0.008 , \end{aligned} \quad (3)$$

which exceed the SM predictions by 3.08σ . The discrepancy shows the lepton universality violation. If we allow anomalous τ couplings then one can easily enhance the $R(D^{(*)})$ values, as in [13]. There have been many attempts to explain the discrepancy in various NP models, like leptoquark models [14–20], composite models [21–24], extra dimensions [25–29], etc. [30–32].

In addition to $R(D^{(*)})$, there are other observables related to the polarizations in $B \rightarrow D^{(*)}\tau\nu$ decays., involving τ as well as D^* polarizations. Firstly, the polarization asymmetry of τ is defined as

$$P_\tau(D^{(*)}) \equiv \frac{\Gamma_\tau^{D^{(*)}}(+)-\Gamma_\tau^{D^{(*)}}(-)}{\Gamma_\tau^{D^{(*)}}(+)+\Gamma_\tau^{D^{(*)}}(-)} , \quad (4)$$

where $\Gamma_\tau^{D^{(*)}}(\pm)$ is the decay width corresponding to (\pm) τ helicity. Expected values from the SM are [33, 34]

$$P_\tau(D)_{\text{SM}} = 0.325 \pm 0.009 , \quad P_\tau(D^*)_{\text{SM}} = -0.497 \pm 0.013 . \quad (5)$$

Experimentally the measured value is [7, 8]

$$P_\tau(D^*) = -0.38 \pm 0.51_{-0.16}^{+0.21} . \quad (6)$$

Secondly, the longitudinal D^* polarization is given by

$$F_L(D^*) \equiv \frac{\Gamma(B \rightarrow D_L^* \tau \nu)}{\Gamma(B \rightarrow D^* \tau \nu)} . \quad (7)$$

The SM prediction is [35]

$$F_L(D^*)_{\text{SM}} = 0.46 \pm 0.04 , \quad (8)$$

which is smaller than the Belle's measurement [36]

$$F_L(D^*) = 0.60 \pm 0.08 \pm 0.035 . \quad (9)$$

Among other NP models, the unparticle(\mathcal{U}) scenario is quite interesting and unique [37, 38]. Unparticles are low-energy realization of a scale-invariant hidden sector at some high-energy scale. In the context of the effective field theory, unparticles behave like a fractional number of particles. Usually unparticles contribute in the form of $\lambda_{\mathcal{U}}^2 (M_{\text{EW}}^2/\Lambda_{\mathcal{U}}^2)^{d_{\mathcal{U}}}$, where M_{EW} is the electroweak scale, $\lambda_{\mathcal{U}}$ is some relevant coupling, $\Lambda_{\mathcal{U}}$ is a new high-energy scale for the scale invariance, and $d_{\mathcal{U}}$ is the scaling dimension of the unparticle operators. Typical NP involves ordinary particles with a definite integer of $d_{\mathcal{U}}$ while for unparticles $d_{\mathcal{U}}$ is a free parameter, which makes the scenario more interesting. One can suppress or enhance the NP effects by not only the new scale $\Lambda_{\mathcal{U}}$ but also $d_{\mathcal{U}}$. In general scalar and vector unparticles can contribute together. But as for the vector unparticles the lower bound of the associated scaling dimension is larger than that for the scalar unparticles, resulting in more suppressions of $(M_{\text{EW}}^2/\Lambda_{\mathcal{U}}^2)$. Unparticles can affect the B physics in many ways [39–41], for example, B_s - \bar{B}_s mixing [42–45] (for meson mixing, see [46, 47]), and $B_s \rightarrow \mu^+ \mu^-$ [48], etc. These are included as constraints in this analysis.

The paper is organized as follows. In the next section, unparticle descriptions are given for the relevant observables. Our results and discussions appear in Sec. III. We conclude in Sec. IV.

II. UNPARTICLES AND OBSERVABLES

The relevant Lagrangian involving scalar unparticles \mathcal{O}_U and vector ones \mathcal{O}_U^μ is given by [41, 48]

$$\mathcal{L}_U = \sum_f \left[\frac{c_S^{f'f}}{\Lambda_U^{d_U}} \bar{f}' \gamma_\mu (1 - \gamma_5) f \partial^\mu \mathcal{O}_U + \frac{c_V^{f'f}}{\Lambda_U^{d_V-1}} \bar{f}' \gamma_\mu (1 - \gamma_5) f \mathcal{O}_U^\mu \right], \quad (10)$$

where $c_{S,V}^{L(R),f'f}$ are dimensionless couplings, and $d_U(d_V)$ is the scaling dimension of $\mathcal{O}_U(\mathcal{O}_U^\mu)$. Note that we only consider the left-handed currents for simplicity. The unitarity constraint requires that $d_U \geq 1$ and $d_V \geq 3$ [38]. Typically the scalar and vector contributions amount to $\sim (M_{\text{EW}}^2/\Lambda_U^2)^{d_U}$ and $\sim (M_{\text{EW}}^2/\Lambda_U^2)^{d_V-1}$, respectively. One can expect that effects of vector unparticles are very suppressed compared to those of scalar ones due to the unitarity constraints [48]. In this analysis we put for simplicity $d_U = 1 + \epsilon_U$ and $d_V = 3 + \epsilon_U$ with $0 \leq \epsilon_U \leq 1$.

The effective Hamiltonian for $b \rightarrow c\ell\nu$ with unparticles is

$$\mathcal{H}_{\text{eff}} = \frac{4G_F}{\sqrt{2}} V_{cb} \sum_{\ell=\mu,\tau} \left[(1 + C_V^{L,\ell}) \mathcal{O}_V^{L,\ell} + C_S^{L,\ell} \mathcal{O}_S^{L,\ell} + C_S^{R,\ell} \mathcal{O}_S^{R,\ell} \right], \quad (11)$$

where the operators $\mathcal{O}_{V,S}^\ell$ are defined by

$$\mathcal{O}_V^{L,\ell} = (\bar{c}_L \gamma^\mu b_L) (\bar{\ell}_L \gamma_\mu \nu_{\ell L}), \quad (12)$$

$$\mathcal{O}_S^{L,\ell} = (\bar{c}_R b_L) (\bar{\ell}_R \nu_{\ell L}), \quad (13)$$

$$\mathcal{O}_S^{R,\ell} = (\bar{c}_L b_R) (\bar{\ell}_R \nu_{\ell L}). \quad (14)$$

The Wilson coefficients are (putting $c_{S,V}^{cb} \equiv c_{S,V}^q$ and $c_{S,V}^{\ell\nu} \equiv c_{S,V}^\ell$)

$$2\sqrt{2}G_F m_B^2 V_{cb} C_V^{L,\ell} = \frac{-A_{d_V} e^{-i\epsilon_U \pi}}{2 \sin \epsilon_U \pi} \left(\frac{m_B}{\Lambda_U} \right)^{2\epsilon_U+4} c_V^q c_V^\ell, \quad (15)$$

$$2\sqrt{2}G_F m_B^2 V_{cb} C_S^{L,\ell} = \frac{-A_{d_S} e^{-i\epsilon_U \pi}}{2 \sin \epsilon_U \pi} \left(\frac{m_B}{\Lambda_U} \right)^{2\epsilon_U+2} \left(\frac{m_\ell m_c}{m_B^2} \right) c_S^q c_S^\ell, \quad (16)$$

$$2\sqrt{2}G_F m_B^2 V_{cb} C_S^{R,\ell} = \frac{A_{d_S} e^{-i\epsilon_U \pi}}{2 \sin \epsilon_U \pi} \left(\frac{m_B}{\Lambda_U} \right)^{2\epsilon_U+2} \left(\frac{m_\ell m_b}{m_B^2} \right) c_S^q c_S^\ell, \quad (17)$$

where

$$A_{d_U} = \frac{16\pi^{5/2}}{(2\pi)^{2d_U}} \frac{\Gamma(d_U + 1/2)}{\Gamma(d_U - 1)\Gamma(2d_U)}, \quad (18)$$

$$\phi_U = (d_U - 2)\pi. \quad (19)$$

Here we have neglected the terms of $\mathcal{O}(m_B^2/\Lambda_U^2)$ in $C_S^{L,R}$. They involve vector couplings of $c_V^q c_V^\ell$. Note that the couplings appear in combined forms of $c_{S,V}^q c_{S,V}^\ell$. Numerically the observables for $B \rightarrow D^{(*)} \ell \nu_\ell$ decays are (at $\mu = m_b$ scale) [49–51]

$$R(D^{(*)}) = R_{\text{SM}}(D^{(*)}) \frac{2 \left[1 + r_{\tau,\mathcal{U}}^{(*)} \right]}{1 + \left[1 + r_{\mu,\mathcal{U}}^{(*)} \right]}, \quad (20)$$

where

$$\begin{aligned} 1 + r_{\ell,\mathcal{U}} &= \left| 1 + C_V^{L,\ell} \right|^2 + 1.54 \text{Re} \left[\left(1 + C_V^{L,\ell} \right) \left(C_S^{L,\ell} + C_S^{R,\ell} \right)^* \right] + 1.09 \left| C_S^{L,\ell} + C_S^{R,\ell} \right|^2, \\ 1 + r_{\ell,\mathcal{U}}^* &= \left| 1 + C_V^{L,\ell} \right|^2 + 0.13 \text{Re} \left[\left(1 + C_V^{L,\ell} \right) \left(C_S^{R,\ell} - C_S^{L,\ell} \right)^* \right] + 0.05 \left| C_S^{R,\ell} - C_S^{L,\ell} \right|^2 \end{aligned} \quad (21)$$

and

$$P_\tau(D) = 1 - 0.68 \frac{\left| 1 + C_V^{L,\tau} \right|^2}{1 + r_{\tau,\mathcal{U}}}, \quad (22)$$

$$P_\tau(D^*) = 1 - 1.49 \frac{\left| 1 + C_V^{L,\tau} \right|^2}{1 + r_{\tau,\mathcal{U}}^*}, \quad (23)$$

$$F_L(D^*) = 1 - 0.54 \frac{\left| 1 + C_V^{L,\tau} \right|^2}{1 + r_{\tau,\mathcal{U}}^*}. \quad (24)$$

III. RESULTS AND DISCUSSIONS

The experimental data are summarized in Table I [29]. For the uncertainties of LHCb(2017), see discussion in [11]. The χ^2 is defined by

$$\chi^2 \equiv \sum_{i,j} \left[\mathcal{O}_i^{\text{exp}} - \mathcal{O}_i^{\text{th}} \right] \mathcal{C}_{ij}^{-1} \left[\mathcal{O}_j^{\text{exp}} - \mathcal{O}_j^{\text{th}} \right], \quad (25)$$

where $\mathcal{O}_i^{\text{exp}}$ are the experimental data in Table I and $\mathcal{O}_i^{\text{th}}$ are the theoretical calculations from Eqs.(20)-(24). Here \mathcal{C}_{ij} are the correlation matrix elements. There are relevant constraints from flavor physics. We include B_s - \bar{B}_s mixing[42, 52, 53], $B \rightarrow D^+ D^-$ decay[54], $B_s \rightarrow \mu^+ \mu^-$ decay, and $B_c \rightarrow \tau \nu$ decay. The first two involve only quark couplings $c_{S,V}^q$ while others do $c_{S,V}^q c_{S,V}^\ell$. For these constraints we only consider the scalar couplings for simplicity since they are dominant. For B_s - \bar{B}_s mixing, the mass difference ΔM_s is given by

$$\Delta M_s = 2 |M_{12}^{\text{SM}}| |\Delta_s| = \Delta M_s^{\text{SM}} |\Delta_s| \quad (26)$$

	$R(D)$	$R(D^*)$
BABAR	$0.440 \pm 0.058 \pm 0.042$	$0.332 \pm 0.024 \pm 0.018$ [3]
Belle(2015)	$0.375 \pm 0.064 \pm 0.026$	$0.293 \pm 0.038 \pm 0.015$ [4]
Belle(2016)	–	$0.302 \pm 0.030 \pm 0.011$ [5]
Belle(2017)	–	$0.276 \pm 0.034^{+0.029}_{-0.026}$ [6]
Belle(2017)	–	$0.270 \pm 0.035^{+0.028}_{-0.025}$ [7, 8]
Belle(2019)	$0.307 \pm 0.037 \pm 0.016$	$0.283 \pm 0.018 \pm 0.014$ [9]
LHCb(2015)	–	$0.336 \pm 0.027 \pm 0.030$ [10]
LHCb(2017)	–	$0.291 \pm 0.019 \pm 0.026 \pm 0.013$ [11]
	$P_\tau(D^*)$	$F_L(D^*)$
Belle(2017)	$-0.38 \pm 0.51^{+0.21}_{-0.16}$ [7, 8]	–
Belle(2019)	–	$0.60 \pm 0.08 \pm 0.04$ [36]

TABLE I. Summary of experimental data for $R(D^{(*)})$, $P_\tau(D^{(*)})$ and $F_L(D^{(*)})$. The uncertainties are $\pm(\text{statistical})\pm(\text{systematic})$. The correlations between $R(D)$ and $R(D^*)$ for BABAR, Belle(2015), and Belle(2019) results are -0.31 , -0.50 and -0.51 , respectively [12].

where

$$M_{12}^{\text{SM}} = \frac{G_F^2 m_W^2}{12\pi^2} (V_{ts}^* V_{tb})^2 m_{B_s} B_{B_s} f_{B_s}^2 \eta_{B_s} S_0(x_t) . \quad (27)$$

Here $S_0(x_t \equiv m_t^2/m_W^2)$ is the Inami-Lim function, and other hadronic parameters can be found in [42, 45]. And Δ_s is defined by

$$\Delta_s = 1 + (c_S^q)^2 f_s(d_U) \cot(d_U \pi) - i (c_S^q)^2 f_s(d_U) , \quad (28)$$

where

$$f_s(d_U) \equiv \frac{1}{M_{12}^{\text{SM}}} \frac{2\pi^{5/2}}{(2\pi)^{2d_U}} \frac{\Gamma(d_U + 1/2)}{\Gamma(d_U - 1)\Gamma(2d_U)} \left(\frac{f_{B_s}^2}{m_{B_s}}\right) \left(\frac{m_{B_s}^2}{\Lambda_U^2}\right)^{d_U} \frac{5}{3} . \quad (29)$$

The decay rate difference is [42]

$$\Delta\Gamma_s = 2|\Gamma_{12,s}| \cos(\phi_s^{\text{SM}} + \phi_s^\Delta) = (0.096 \pm 0.039) \text{ ps}^{-1} \times \cos(\phi_s^{\text{SM}} + \phi_s^\Delta) , \quad (30)$$

where $\phi_s^{\text{SM}(\Delta)}$ is the phase of the SM(Δ_s) contribution. Another observable is the CP asymmetry parameter [42]

$$a_{f_s}^s = \text{Im} \frac{\Gamma_{12,s}}{M_{12}} . \quad (31)$$

We use the following experimental data [55]

$$\Delta M_s = 17.757 \pm 0.021 \text{ ps}^{-1} , \quad (32)$$

$$\Delta \Gamma_s = 0.090 \pm 0.005 \text{ ps}^{-1} , \quad (33)$$

$$a_{f_s}^s = (0.6 \pm 2.8) \times 10^{-3} . \quad (34)$$

As for $B \rightarrow DD$ decays, the branching ratio is [54]

$$\text{Br}(B \rightarrow D^+ D^-) = \text{Br}_{DD}^{\text{SM}} f_{\Delta_{DD}} , \quad (35)$$

where $\text{Br}_{DD}^{\text{SM}}$ is the SM contribution, and

$$f_{\Delta_{DD}} = |1 + \Delta_{DD} e^{-i\phi_U} e^{-i\phi_w}| , \quad (36)$$

$$\Delta_{DD} = \frac{|c_S^q|^2}{a_1 |V_{cb} V_{cd}|} \frac{A_{d_U}}{2 \sin(d_U \pi)} \left(\frac{m_b + m_c}{m_c} \right) \frac{\sqrt{2}}{G_F \Lambda_U^2} \left(\frac{m_D^2}{\Lambda_U^2} \right)^{d_U - 1} . \quad (37)$$

The CP asymmetric parameters C_{DD} and S_{DD} are given by

$$C_{DD} = \frac{2\Delta_{DD}}{\bar{f}_{DD}} \sin \phi_w \sin(d_U \pi) , \quad (38)$$

$$S_{DD} = \frac{-1}{\bar{f}_{DD}} [\sin 2\beta_0 + 2\Delta_{DD} \cos(d_U \pi) \sin(2\beta_0 - \phi_w) + \Delta_{DD}^2 \sin(2\beta_0 - 2\phi_w)] , \quad (39)$$

where

$$\bar{f}_{DD} = 1 + 2\Delta_{DD} \cos \phi_w \cos(d_U \pi) + \Delta_{DD}^2 , \quad (40)$$

and β_0 is the relevant CKM phase and ϕ_w is the weak phase. We fix $\phi_w = 3\pi/2$ in this analysis. For details, see [42]. Experimental data are [56]

$$\text{Br}(B \rightarrow D^+ D^-) = (2.12 \pm 0.16 \pm 0.18) \times 10^{-4} , \quad (41)$$

$$C_{DD} = -0.43 \pm 0.16 \pm 0.05 , \quad (42)$$

$$S_{DD} = -1.06_{-0.14}^{+0.21} \pm 0.08 . \quad (43)$$

Now consider $B_s \rightarrow \mu\mu$ decay. The measured branching ratio is

$$\text{Br}(B_s \rightarrow \mu^+ \mu^-) = (3.2_{-1.2}^{+1.5}) \times 10^{-9} , \quad (44)$$

Theoretically the branching ratio can be written as

$$\text{Br}(B_s \rightarrow \mu\mu) = \text{Br}_{\text{SM}} \cdot |P|^2 , \quad (45)$$

$R(D)$	$R(D^*)$	$P_\tau(D)$	$P_\tau(D^*)$	$F_L(D^*)$	$\text{Br}(B_c \rightarrow \tau\nu)$	$\chi_{\min}^2/\text{d.o.f.}$
0.371	0.266	0.452	-0.445	0.476	7.87×10^{-2}	2.22

TABLE II. Best-fit values.

where Br_{SM} is the SM prediction,

$$\text{Br}_{\text{SM}} = (3.23 \pm 0.27) \times 10^{-9} , \quad (46)$$

and

$$P = 1 + \frac{m_{B_s}^2}{2m_\mu} \frac{m_b}{m_b + m_s} \frac{C_P}{C_{10}^{\text{SM}}} . \quad (47)$$

Here the coefficients C_{10}^{SM} and C_P are given by

$$C_{10}^{\text{SM}} = -\frac{1}{\sin^2 \theta_W} \eta_Y Y_0(x_t) , \quad (48)$$

$$C_P = \frac{\sqrt{2}\pi}{G_F \alpha (V_{tb} V_{ts}^*)} \frac{A_{d\mathcal{U}} e^{i\phi_{\mathcal{U}}}}{\sin d_{\mathcal{U}} \pi} \left(\frac{m_{B_s}}{\Lambda_{\mathcal{U}}} \right)^{2d_{\mathcal{U}}} \left(\frac{2m_\mu}{m_{B_s}^4} \right) (c_S^q \cdot c_S^\ell)^* , \quad (49)$$

where $x_t = m_t^2/m_W^2$, $Y(x) = \eta_Y Y_0(x)$, and

$$Y_0(x) = \frac{x}{8} \left[\frac{x-4}{x-1} + \frac{3x}{(x-1)^2} \ln x \right] , \quad \eta_Y = 1.0113 . \quad (50)$$

For more details, see [48].

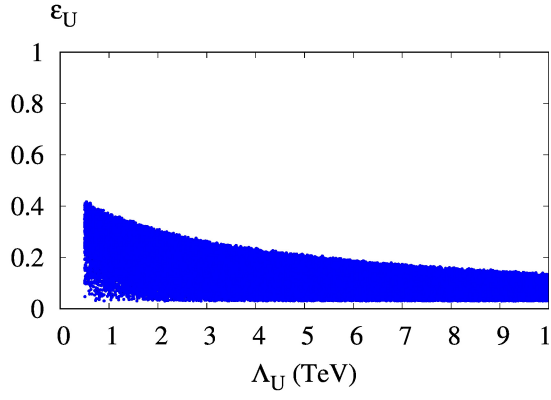
Finally, the branching ratio of $B_c \rightarrow \tau\nu$ decay is

$$\text{Br}(B_c \rightarrow \tau\nu) = 0.02 \left(\frac{f_{B_c}}{0.43 \text{ GeV}} \right)^2 \left| 1 + C_V^{L,\tau} + 4.3(C_S^{R,\tau} - C_S^{L,\tau}) \right|^2 . \quad (51)$$

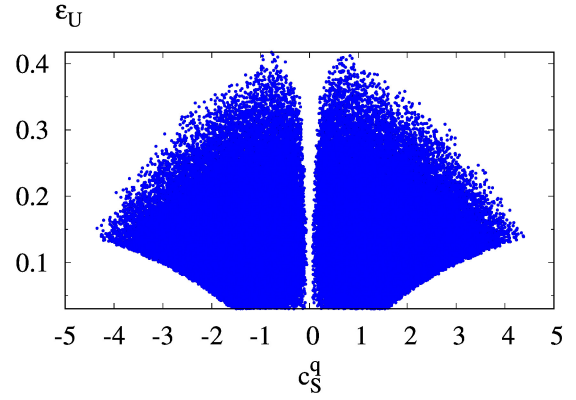
Note that large $R(D^{(*)})$ favors large $C_V^{L,\tau}$ or $(C_S^{R,\tau} - C_S^{L,\tau})$, which makes $\text{Br}(B_c \rightarrow \tau\nu)$ larger. It means that small $\text{Br}(B_c \rightarrow \tau\nu)$ would provide severe constraints on model parameters [57]. The predicted upper bound ranges from 10% to 60% [58]. In this analysis we require the branching ratio less than 30%.

For the fitting, we simply put $c_V^{q,\ell} = c_S^{q,\ell}$. As mentioned before, the vector \mathcal{U} contribution is highly suppressed. We found that $C_V^{L,\tau}$ is smaller than $C_S^{L(R),\tau}$ by a few orders. This is due to the factor of $m_B^2/\Lambda_{\mathcal{U}}^2 \sim \mathcal{O}(10^{-6})$ for $\Lambda_{\mathcal{U}} \simeq 1 \text{ TeV}$. Thus the couplings $c_V^{q,\ell}$ must be of order $\mathcal{O}(10^3)$ in order to compete the scalar contributions.

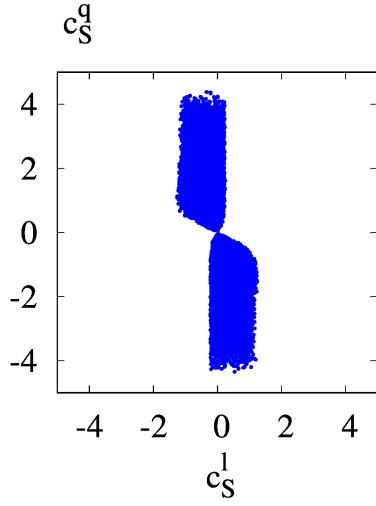
Our results are summarized in Table II where the best-fit values for the minimum χ^2 are given. The best-fit value of $R(D)$ is quite larger than the SM prediction, and that of



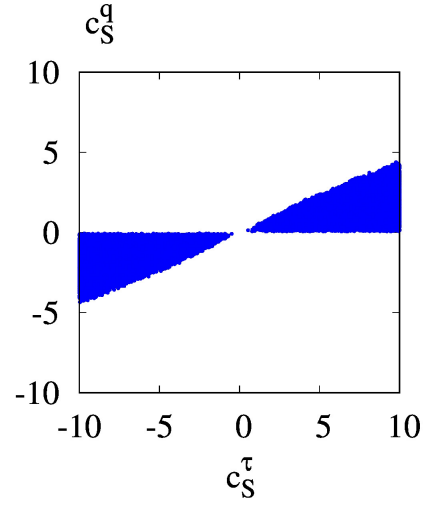
(a)



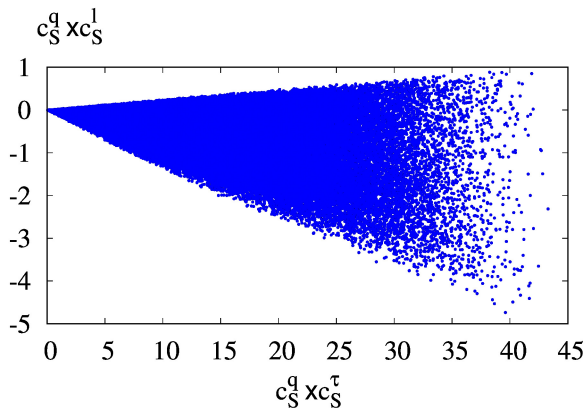
(b)



(c)



(d)



(e)

FIG. 1. Parameter spaces allowed at the 2σ level for (a) ϵ_U vs Λ_U (TeV), (b) ϵ_U vs c_S^q , (c) c_S^q vs c_S^ℓ , (d) c_S^q vs c_S^τ , and (e) $c_S^q c_S^\ell$ vs $c_S^q c_S^\tau$, where $\ell = e, \mu$.

$\text{Br}(B_c \rightarrow \tau\nu)$ is below 10%. Figure 1 shows the allowed region of model parameters at the 2σ level. The pattern shown in Fig. 1 (a) is typical in unparticle scenario. Unparticle contributions appear in the form of $C_U (m_B^2/\Lambda_U^2)^{\epsilon_U}$ where C_U is some combination of the relevant couplings. For large values of Λ_U , large ϵ_U suppresses the new contribution too much to provoke meaningful effects. The CMS collaboration had put a lower limit on Λ_U with respect to ϵ_U at high-energy collisions [59]. The results are for larger values of $c_S^{q,\ell} \sim \mathcal{O}(10^3)$ where Λ_U must be large enough to moderate the unparticle effects. As discussed in [48] the results are consistent with ours.

The quark coupling c_S^q in relation with ϵ_U is plotted in Fig. 1 (b). Figure 1 (c) shows the quark coupling vs lepton one. For these couplings $B \rightarrow D^+D^-$ and $B_s \rightarrow \mu^+\mu^-$ decays provide severe bounds on c_S^q and c_S^ℓ , respectively. $B_s\text{-}\bar{B}_s$ mixing could also constrain the c_S^q coupling, but the result is rather weak because uncertainties in the experimental data are still large.

In Fig. 1 (d) c_S^q vs c_S^τ is shown. Large values of c_S^τ are favored, as expected. Note that a small c_S^q multiplied by a small c_S^τ results in small Wilson coefficients for $R(D^{(*)})$, which are disfavored by experimental data. Figures 1 (c) and 1 (d) show that c_S^ℓ favors the opposite sign c_S^q while c_S^τ does the same sign c_S^q . Note that the couplings appear in the form of $c_S^q c_S^{\ell,\tau}$ in the Wilson coefficients. As a result, $c_S^q c_S^\tau$ is positive while $c_S^q c_S^\ell$ is mostly negative, as in Fig. 1 (e). We found that the value of χ^2 gets smaller when $c_S^q c_S^\ell$ approaches to zero.

On the other hand, we found that $\text{Br}(B_c \rightarrow \tau\nu)$ puts no significant bounds on c_S^τ . We found that requiring $\text{Br}(B_c \rightarrow \tau\nu) < 30\%$ has almost no difference from $\text{Br}(B_c \rightarrow \tau\nu) < 10\%$. All the allowed points satisfy $\text{Br}(B_c \rightarrow \tau\nu) < 10\%$, as shown in Fig. 2 (a).

Some comments are in order for $b \rightarrow s\gamma$, which provides significant constraints on flavor physics. For unparticles, $b \rightarrow s\gamma$ constrains the quark couplings as studied in [60]. The analysis of [60] was done at fixed $\Lambda_U = 1$ TeV. According to [60], smaller quark couplings are allowed for smaller ϵ_U , and for larger values of ϵ_U the constraints become very weak. This is due to the suppression factor of $(M_{\text{EW}}^2/\Lambda_U^2)^{\epsilon_U}$. For example, the product of scalar quark couplings $\lambda_{ss}^{YD} \lambda_{bs}^{YD}$ has a bound of -0.0026 at $\epsilon_U = 0.1$ [60]. In our language, $c_S^q = (v/m_q) \lambda_{qq'}^{YD}$ where v is the Higgs vacuum expectation value. Thus the bound of [60] would not be strong for our analysis.

Figure 2 shows the ranges of observables at the 2σ level. Our predictions for $\text{Br}(B_c \rightarrow \tau\nu)$ vs $R(D)$ are given in Fig. 2 (a). Note that keeping $\text{Br}(B_c \rightarrow \tau\nu)$ small and making $R(D)$

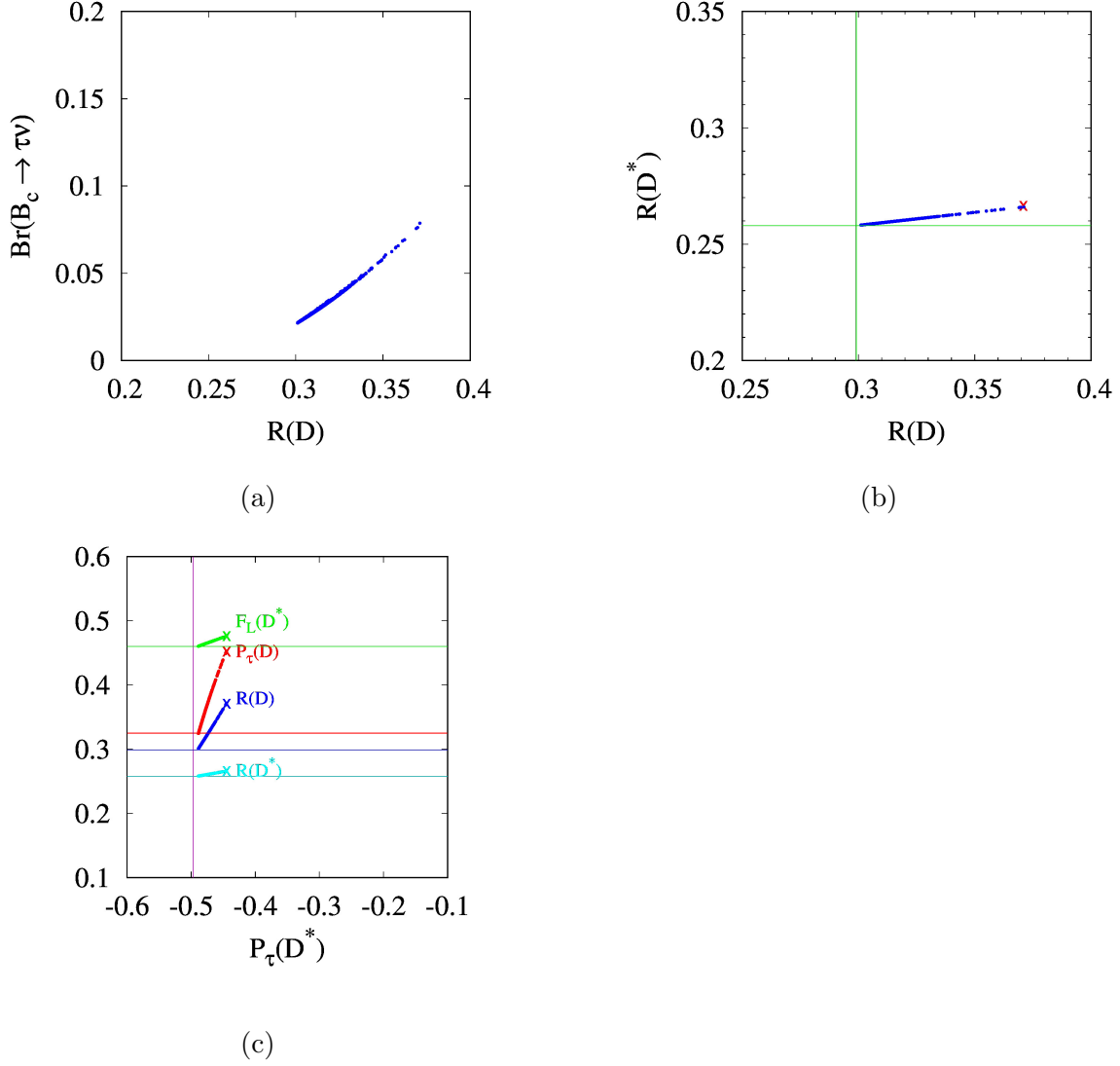


FIG. 2. Predicted ranges of observables at the 2σ level. In (a) $\text{Br}(B_c \rightarrow \tau\nu)$ vs $R(D)$; in (b) $R(D^*)$ vs $R(D)$; in (c) $R(D^*)$, $P_\tau(D)$, and $F_L(D)$ vs $P_\tau(D^*)$. In (b) and (c) vertical and horizontal lines are the SM predictions while the marks "x" denote the best-fit values.

large enough to fit the data is possible in our scenario. As mentioned before, requiring small branching ratio for $B_c \rightarrow \tau\nu$ is not powerful for the model parameters. We found that the constraint from $B \rightarrow D^+D^-$ decay already suppresses $\text{Br}(B_c \rightarrow \tau\nu)$ strongly. In Figs. 2 (b) and (c), the marks "x" represent the best-fit values and the straight lines are the central values of the SM predictions. As seen in Fig. 2 (b), $R(D^*)_{\text{SM}}$ is at the edge of our allowed range while $R(D)_{\text{SM}}$ is outside. And the best-fit values lie in the far side of the region. In Fig. 2 (c) $R(D^*)$, $P_\tau(D)$, and $F_L(D)$ vs $P_\tau(D^*)$ are provided. We find that the SM

prediction of $P_\tau(D^*)$ lies outside of our allowed region.

IV. CONCLUSIONS

In conclusion, we have analyzed the B anomalies in the unparticle scenario. We included the scalar and vector unparticles, and found that vector contributions are a few orders of magnitude smaller than scalar ones. We implemented the global fit to the relevant observables by minimizing χ^2 . Various constraints are imposed on the model parameters. Compared to our previous works [45, 48], $\chi^2_{\min}/\text{d.o.f.}$ in this work is slightly larger than before. It's because $B \rightarrow D^+ D^-$ decay puts quite a strong constraint on the quark coupling. As discussed in [29], a similar situation could occur in the nmUED model when the quark sector is severely constrained. On the other hand, $\text{Br}(B_c \rightarrow \tau \nu)$ might not be a strong restriction to the model parameters. One can safely keep the branching ratio at low values. This was also true for our previous works [29, 41]. We expect more data on anomalous observables could test the unparticle scenario further in near future.

-
- [1] Y. Amhis *et al.* [HFLAV Collaboration], Eur. Phys. J. C **77**, no. 12, 895 (2017).
 - [2] J. P. Lees *et al.* [BaBar Collaboration], Phys. Rev. Lett. **109**, 101802 (2012).
 - [3] J. P. Lees *et al.* [BaBar Collaboration], Phys. Rev. D **88**, no. 7, 072012 (2013).
 - [4] M. Huschle *et al.* [Belle Collaboration], Phys. Rev. D **92**, no. 7, 072014 (2015).
 - [5] Y. Sato *et al.* [Belle Collaboration], Phys. Rev. D **94**, no. 7, 072007 (2016).
 - [6] S. Hirose [Belle Collaboration], Nucl. Part. Phys. Proc. **287-288**, 185 (2017).
 - [7] S. Hirose *et al.* [Belle Collaboration], Phys. Rev. Lett. **118**, no. 21, 211801 (2017).
 - [8] S. Hirose *et al.* [Belle Collaboration], Phys. Rev. D **97**, no. 1, 012004 (2018).
 - [9] A. Abdesselam *et al.* [Belle Collaboration], arXiv:1904.08794 [hep-ex].
 - [10] R. Aaij *et al.* [LHCb Collaboration], Phys. Rev. Lett. **115**, no. 11, 111803 (2015) Addendum: [Phys. Rev. Lett. **115**, no. 15, 159901 (2015)].
 - [11] R. Aaij *et al.* [LHCb Collaboration], Phys. Rev. D **97**, no. 7, 072013 (2018).
 - [12] Average of $R(D)$ and $R(D^*)$ for Spring 2019, Heavy Flavor Averaging Group, <https://hflav-eos.web.cern.ch/hflav-eos/semi/spring19/html/RDsDsstar/RDRDs.html>

- [13] J. P. Lee, Phys. Rev. D **96**, no. 5, 055005 (2017).
- [14] I. Doršner, S. Fajfer, N. Košnik and I. Nišandžić, JHEP **1311**, 084 (2013).
- [15] R. Alonso, B. Grinstein and J. Martin Camalich, JHEP **1510**, 184 (2015).
- [16] M. Bauer and M. Neubert, Phys. Rev. Lett. **116**, no. 14, 141802 (2016).
- [17] R. Barbieri, G. Isidori, A. Pattori and F. Senia, Eur. Phys. J. C **76**, no. 2, 67 (2016).
- [18] L. Di Luzio, A. Greljo and M. Nardecchia, Phys. Rev. D **96**, no. 11, 115011 (2017).
- [19] L. Calibbi, A. Crivellin and T. Li, Phys. Rev. D **98**, no. 11, 115002 (2018).
- [20] D. Bečirević, I. Doršner, S. Fajfer, N. Košnik, D. A. Faroughy and O. Sumensari, Phys. Rev. D **98**, no. 5, 055003 (2018).
- [21] R. Barbieri, C. W. Murphy and F. Senia, Eur. Phys. J. C **77**, no. 1, 8 (2017).
- [22] D. Buttazzo, A. Greljo, G. Isidori and D. Marzocca, JHEP **1711**, 044 (2017).
- [23] M. Bordone, C. Cornella, J. Fuentes-Martin and G. Isidori, Phys. Lett. B **779**, 317 (2018).
- [24] S. Matsuzaki, K. Nishiwaki and K. Yamamoto, [arXiv:1903.10823 [hep-ph]].
- [25] E. Megias, M. Quiros and L. Salas, JHEP **1707**, 102 (2017).
- [26] E. Megias, M. Quiros and L. Salas, Phys. Rev. D **96**, no. 7, 075030 (2017).
- [27] G. D'Ambrosio and A. M. Iyer, Eur. Phys. J. C **78**, no. 6, 448 (2018).
- [28] M. Blanke and A. Crivellin, Phys. Rev. Lett. **121**, no. 1, 011801 (2018).
- [29] J. P. Lee, Phys. Rev. D **100**, no.7, 075005 (2019).
- [30] X. W. Kang, T. Luo, Y. Zhang, L. Y. Dai and C. Wang, Eur. Phys. J. C **78**, no. 11, 909 (2018).
- [31] Z. R. Huang, Y. Li, C. D. Lu, M. A. Paracha and C. Wang, Phys. Rev. D **98**, no. 9, 095018 (2018).
- [32] D. Bardhan and D. Ghosh, Phys. Rev. D **100**, no. 1, 011701 (2019) doi:10.1103/PhysRevD.100.011701 [arXiv:1904.10432 [hep-ph]].
- [33] M. Tanaka and R. Watanabe, Phys. Rev. D **82**, 034027 (2010).
- [34] M. Tanaka and R. Watanabe, Phys. Rev. D **87**, no. 3, 034028 (2013).
- [35] A. K. Alok, D. Kumar, S. Kumbhakar and S. U. Sankar, Phys. Rev. D **95**, no. 11, 115038 (2017).
- [36] A. Abdesselam *et al.* [Belle Collaboration], arXiv:1903.03102 [hep-ex].
- [37] H. Georgi, Phys. Rev. Lett. **98**, 221601 (2007); Phys. Lett. B **650**, 275 (2007).
- [38] B. Grinstein, K. A. Intriligator and I. Z. Rothstein, Phys. Lett. B **662**, 367 (2008).

- [39] C. H. Chen and C. Q. Geng, Phys. Rev. D **76**, 115003 (2007).
- [40] R. Mohanta and A. K. Giri, Phys. Lett. B **660**, 376 (2008).
- [41] J. P. Lee, Mod. Phys. Lett. A **34**, no.19, 1950149 (2019).
- [42] A. Lenz, Phys. Rev. D **76**, 065006 (2007); A. Lenz and U. Nierste, JHEP **0706**, 072 (2007).
- [43] R. Mohanta and A. K. Giri, Phys. Rev. D **76**, 075015 (2007).
- [44] J. K. Parry, Phys. Rev. D **78**, 114023 (2008).
- [45] J. -P. Lee, Phys. Rev. D **82**, 096009 (2010).
- [46] X. Q. Li and Z. T. Wei, Phys. Lett. B **651**, 380 (2007).
- [47] S. L. Chen, X. G. He, X. Q. Li, H. C. Tsai and Z. T. Wei, Eur. Phys. J. C **59**, 899 (2009).
- [48] J. -P. Lee, Phys. Rev. D **88**, no. 11, 116003 (2013).
- [49] M. Blanke, A. Crivellin, S. de Boer, T. Kitahara, M. Moscati, U. Nierste and I. Nišandžić, Phys. Rev. D **99**, no. 7, 075006 (2019); arXiv:1905.08253 [hep-ph].
- [50] S. Aoki *et al.*, Eur. Phys. J. C **77**, no. 2, 112 (2017).
- [51] F. U. Bernlochner, Z. Ligeti, M. Papucci and D. J. Robinson, Phys. Rev. D **95**, no. 11, 115008 (2017) Erratum: [Phys. Rev. D **97**, no. 5, 059902 (2018)].
- [52] L. Di Luzio, M. Kirk and A. Lenz, Phys. Rev. D **97**, no. 9, 095035 (2018).
- [53] L. Di Luzio, M. Kirk and A. Lenz, arXiv:1811.12884 [hep-ph].
- [54] R. Zwicky, Phys. Rev. D **77**, 036004 (2008).
- [55] Y. Amhis *et al.* [HFLAV Collaboration], Eur. Phys. J. C **77**, no. 12, 895 (2017).
- [56] M. Rohrken *et al.* [Belle Collaboration], Phys. Rev. D **85**, 091106 (2012).
- [57] R. Alonso, B. Grinstein and J. Martin Camalich, Phys. Rev. Lett. **118**, no. 8, 081802 (2017).
- [58] A. G. Akeroyd and C. H. Chen, Phys. Rev. D **96**, no. 7, 075011 (2017).
- [59] A. M. Sirunyan *et al.* [CMS Collaboration], JHEP **1703**, 061 (2017) Erratum: [JHEP **1709**, 106 (2017)].
- [60] X. G. He and L. Tsai, JHEP **06**, 074 (2008).